The Role of Motion Feedback in Manual Preview Tracking Tasks

João Luís Alexandre Costa de Morais Almeida
jlmoraisalmeida@ist.utl.pt
Instituto Superior Técnico, Lisboa, Portugal
October 2016

***Abstract*—Motion feedback has an important effect in many tasks performed by humans. In this paper, we aim to investigate the role of motion feedback in preview tracking tasks with double integrator dynamics, using results from a human-in-the-loop experiment performed in the SIMONA Research Simulator of the Delft University of Technology. Eight subjects performed the same yaw tracking task with a compensatory and preview display, both with and without motion feedback. System identification techniques and quasi-linear human controller models for preview and motion feedback are used to explain human controller's behavior in tracking tasks. An extension to an existing human preview control model is proposed, in order to model the human in a preview task using motion feedback. It is found that, when motion feedback is available, human controllers adapt their behavior in a similar way for compensatory and preview tasks. Motion feedback allows human controllers to further improve their performance in preview tracking. This research shows for the first time that motion feedback still has an important effect on the human controller behavior, even if visual preview is available.**

I. Introduction

THE topic of manual control has been widely studied in the scientific community. McRuer and his colleagues [1] developed the widely known "crossover model", which models how humans perform a task using a compensatory display. This enables obtaining a mathematical model for humans in a very simple task, where only the error is displayed. Obtaining such a model for more realistic tasks, where more information is present (more visual feedbacks, motion feedback) would allow for a more complete understanding of manual control.

Research has previously been conducted on the role of motion feedback in compensatory tasks ([2], [3], [4], [5], [6], [7]). Not only was motion feedback found to result in improved tracking performance, but also extensions to the crossover model including motion feedback were proposed. The main drawback of the compensatory task is that it translates poorly to real-life tasks. The preview task, in which the future movement of the target is also shown to the human, is closer to what can be seen in the real world, in tasks such as driving a vehicle along a road. Recent research at the Delft University of Technology proposed a new empirical model for this kind of task ([8], [9]). This model allows to understand how humans use preview, by using both feedforward and feedback control.

It is still not clear if human controllers use preview similarly in tasks using motion feedback, and if motion feedback is still beneficial in preview tracking tasks. This paper investigates the role of motion feedback in preview tracking tasks, by analyzing how both feedbacks affect performance, and human tracking behavior.

The main objective of the project is to understand what is the effect of motion feedback, and if we are able to model the human response to it. In order to do this, an experiment will be conducted in the SIMONA Research Simulator (SRS) at the Delft University of Technology. Subjects perform a yaw tracking task using a double integrator controlled element, with compensatory and preview displays, both with and without motion feedback. A number of parametric and non-parametric measures will be calculated in order to understand the influence of motion feedback on preview tasks. Coherence will be calculated as a measure of linearity of the human controller. Error and control output variances will be obtained, and system identification methods will be used to identify the pilot response. The van der El et. al model [8] will be tested to the experimental data, with an extension for the case of preview with motion feedback. The Variance Accounted For (VAF) will be calculated as a measure of the quality of the model fit.

This paper is structured in six sections. In Section II, the control task is presented, along with the models used for compensatory tasks, with and without motion, and preview tasks. An extended model is proposed for the preview tracking task with motion. The description of the human-in-the-loop experiment and the system identification techniques used are presented in Section III. Section IV contains the experiment results, and Section V the discussion of these results. This paper ends with the conclusions in Section VI.

II. Control Task

A. Task Characteristics

The control task considered in this paper is a combined target-tracking and disturbance-rejection task. In a target-tracking task, the human controller is asked to track a target signal, designated by $f_t(t)$, minimizing the error $e(t)$ between the output $x(t)$ and the current target [1]. This output can also be perturbed by a disturbance signal $f_d(t)$, which constitutes the disturbance-rejection part of the task.

In this paper, control tasks performed with compensatory and preview displays are investigated. In the compensatory task, only the error is displayed. In the preview task, the human controller can see the future target signal up to τ_p seconds

ahead. These displays can be seen in Figure 1. Both displays were chosen to have an "inside-out" representation, with a static output marker (a circle) and a moving target. In the compensatory case (Figure 1 (a)), the target is represented by a cross. In the preview case (Figure 1 (b)) the current target is the bottom ($\tau_p = 0$) of the preview line.

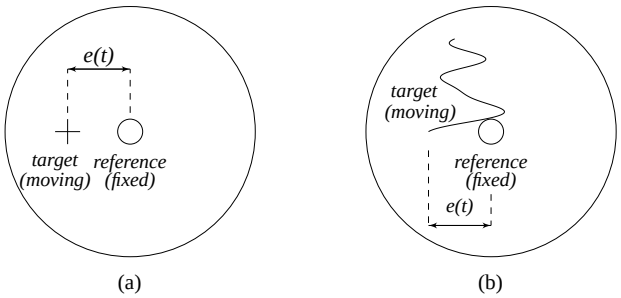

Fig. 1: The compensatory (a) and preview display (b)

The controlled element used in these tracking tasks can take a different number of forms, including models that approach aircraft dynamics to simpler systems such as gain, single integrator and double integrator. In this paper, the focus will be on the double integrator controlled element, since it is the case in which the motion feedback is found to have a larger effect on performance and the highest motion use, according to [4]. The controlled element used in this control task was given by:

$$H_{ce}(j\omega) = \frac{5}{(j\omega)^2} \tag{1}$$

B. Human Controller Modeling in Compensatory Tasks

In the following sections, the human controller modeling approaches in literature will be presented. These approaches follow the control diagram of Figure 2. This diagram presents the McRuer *et al.* in [1] model extended with an additional motion feedback channel (shown in a dashed rectangle) proposed by Hosman [2].

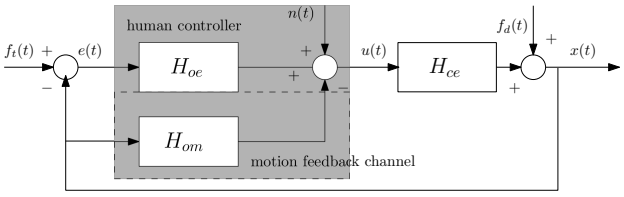

Fig. 2: Compensatory model with motion feedback channel

1) Compensatory Tracking: A compensatory tracking task is defined as a task in which only the current error, $e(t)$, is presented to the human controller. For this type of task, an empirical model has been derived by McRuer *et al.* in [1]. McRuer proposed a quasi-linear model to explain the behavior of the human controller in such a task, in which the operator is described by a linear frequency response function $H_{oe}(j\omega)$, and a non-linear part $n(t)$, the remnant signal.

The proposed model states that humans adapt their control dynamics so that, in the crossover region (around a crossover frequency ω_c), the open-loop describing function approximates a single integrator with a time delay, as in Equation (2) [1].

$$H_{ol}(j\omega) = H_{o_e}(j\omega)H_{ce}(j\omega) = \frac{\omega_c}{j\omega}e^{-j\omega\tau_v} \tag{2}$$

The operator frequency response function $H_{oe}(j\omega)$ is modeled for a double integrator as in Equation (3).

$$H_{oe}(j\omega) = K_e(1 + T_{L,e}j\omega)e^{-\tau_v j\omega}H_{nms}(j\omega) \tag{3}$$

In this model, K_e represents the human controller response gain, $T_{L,e}$ the lead time constant, τ_v the visual time delay and H_{nms} the neuromuscular dynamics. The neuromuscular dynamics are typically modeled [4], as seen in Equation (4), with ω_{nms} the natural frequency of the neuromuscular system and ζ_{nms} the damping ratio.

$$H_{nms}(j\omega) = \frac{\omega_{nms}^2}{(j\omega)^2 + 2\zeta_{nms}\omega_{nms}j\omega + \omega_{nms}^2} \tag{4}$$

2) Role of Motion Feedback: The effect of motion feedback in compensatory tracking tasks is well documented in literature ([2], [3], [4], [5], [6], [7]). Hosman and Van der Vaart [3] found that motion cues significantly improved performance. For the target-following task, a reduction in the target crossover frequency ω_{ct} and an increase in the target phase margin ϕ_{mt} are found. Regarding disturbance rejection, the study found an increase in the disturbance phase margin ϕ_{md} and in the disturbance crossover frequency ω_{cd}. In [5], a compilation of a large number of research studies on the field was obtained, and these findings were found to be a general trend, apart from the phase margins. For both the target and disturbance phase margins, motion was found not to have an effect in this research. According to Hosman [2], the motion feedback is modeled as an extra feedback path, with a frequency response function including the semi-circular canal dynamics:

$$H_{o_m}(j\omega) = (j\omega)^2 H_{scc}(j\omega)K_m e^{-\tau_m j\omega} \tag{5}$$

The most remarkable effect of motion feedback in compensatory tasks is an increase in performance. With motion feedback, human controllers adapt their control strategy, by increasing the error response gain K_e. The lead generated by the motion feedback channel allows human controllers to generate less visual lead, which is shown by the decrease in the lead time constant $T_{L,e}$. The task then becomes easier for the human controller, which is shown by an increase in the disturbance crossover frequency [4], [5].

C. Human Controller Modeling in Preview Tasks

In this paper, a new model for preview tracking tasks is proposed which combines the previous research on compensatory tasks with the van der El *et. al* model [8] for preview tasks without motion feedback. The extension adds an extra feedback path to the preview model, as can be seen in Figure 3. This control diagram shows the hypothesized additional motion channel with a dashed line.

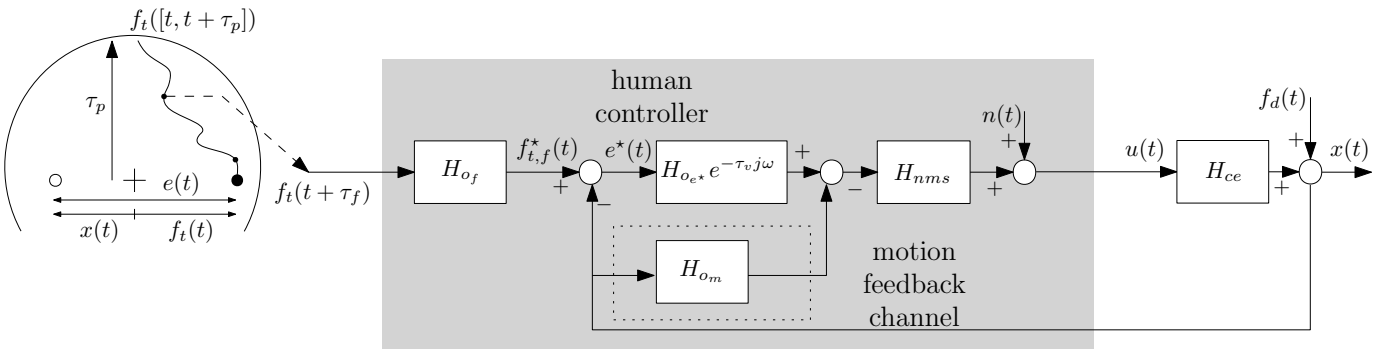

Fig. 3: Preview model proposed by Van der El *et. al* ([8]) including a motion channel

1) Preview Tracking: Van der El *et. al* proposed a model for preview tracking in which the response of the human controller to a previewed target trajectory is captured by a response to two different points ahead: the near-viewpoint $f_{t,n}$ and the far-viewpoint $f_{t,f}$:

$$f_{t,n} = f_t(t+\tau_n) \qquad f_{t,f} = f_t(t+\tau_f) \tag{6}$$

No near-viewpoint was included in the proposed model, since in previous studies it is found to be difficult to determine whether it is actually being used by the human controller [9] and its contribution to the human controller's output is generally small for a double integrator controlled element. This allows to reduce the number of parameters to estimate, yielding lower estimation uncertainties in the remaining parameters, as used in [10].

The far-viewpoint response is modeled as a low-pass filter, as the human controller uses it to track the low frequencies of the target signal:

$$H_{o_f}(j\omega) = K_f \frac{1}{1+T_{l,f}j\omega}, \tag{7}$$

in which K_f is the far-viewpoint gain and $T_{l,f}$ is the far-viewpoint lag time constant.

The human controller responds to an error $e^\star$, defined as the difference between the target filtered by the far-viewpoint dynamics and the controlled element output:

$$E^\star(j\omega) = F^\star_{t,f}(j\omega) - X(j\omega) = H_{o_f}F_t(j\omega) - X(j\omega) \tag{8}$$

The dynamics of the internal-error response resemble the equalization term of compensatory tracking, as can be seen in Equation (9) for a double integrator controlled element.

$$H_{o_{e^\star}}(j\omega) = K_{e^\star}(1+T_{L,e^\star}j\omega) \tag{9}$$

in which $K_{e^\star}$ is the error response gain, $T_{L,e^\star}$ is the lead time constant.

The human controller can respond to the output, the target and the error, in a total of three describing functions. Using two external signals, the target and the disturbance, only two operator describing functions can be identified. The model is then typically restructured to a a two-channel model, with H_{o_t} representing the response to the target and H_{o_x} the response to the controlled element output [8], [9], [10], see Figure 4. These lumped dynamics are defined as:

$$\begin{aligned} H_{o_t}(j\omega) =& [H_{o_f}(j\omega)H_{o_{e^\star}}(j\omega)e^{\tau_f j\omega} \\ &+H_{o_n}(j\omega)e^{\tau_n j\omega}]H_{nms}(j\omega)e^{-\tau_v j\omega} \end{aligned} \tag{10}$$

$$H_{o_x}(j\omega) = H_{o_{e^\star}}(j\omega)H_{nms}(j\omega)e^{-\tau_v j\omega} \tag{11}$$

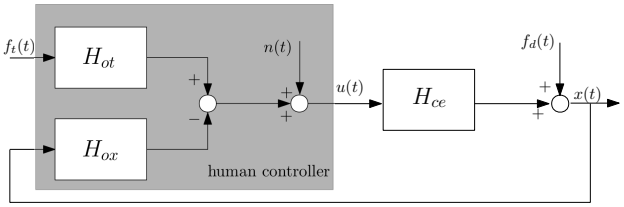

Fig. 4: Model with lumped dynamics in TX (target and output response) form, as in Van der El *et. al* ([8] - [9])

2) Proposed model for Preview with Motion Feedback: The proposed model for preview tracking accounting for motion feedback can be converted to the same lumped structure of Figure 4 by adding the H_{o_m} frequency response function to Equation (11), while there is no change in Equation (10).

$$H_{o_x}(j\omega) = H_{o_{e^\star}}(j\omega)H_{nms}(j\omega)e^{-\tau_v j\omega} + H_{o_m}(j\omega)H_{nms}(j\omega) \tag{12}$$

In this equation, H_{o_m} uses the same structure as Equation (5). The normalized semi-circular canals model was used, as in [11]. This model includes a gain which ensures the model has an unitary absolute value at 1 rad/s.

$$H_{scc}(j\omega) = \frac{5.97(0.11j\omega+1)}{(5.9j\omega+1)(0.005j\omega+1)} \tag{13}$$

It should be noted that the proposed model doesn't introduce a large change in the existing preview model: in fact, the H_{o_m} equation can be simplified over a range of frequencies to:

$$H_{o_m}(j\omega) = |(j\omega)|K_m e^{-\tau_m j\omega} \tag{14}$$

On the other hand, for a double integrator, $H_{o_{e^\star}}$ including the visual time delay is given by:

$$H_{o_{e^\star}} = K_{e^\star}e^{-\tau_v j\omega} + K_{e^\star}T_{L,e^\star}j\omega e^{-\tau_v j\omega} \tag{15}$$

It can be seen that the second term of Equation (15) has the same structure of the additional H_{o_m} path in the proposed model. It can then be expected there is undesired redundancy in the proposed model, which may lead to problems in the identification of its parameters.

III. Method

A. Independent Variables

The experiment considered two independent variables: the display type and the presence of motion feedback. The displays had either compensatory or preview configuration, see Figure 1. The motion feedback was either off or on. A full-factorial design was used, so all combinations of the independent variables were tested by each participant. This yields a total of four conditions, as it can be seen in Table I.

TABLE I: Experimental conditions definition

	Motion off	*Motion on*
Compensatory	C	CM
Preview	P	PM

B. Apparatus

The experiment was conducted in the SIMONA Research Simulator (SRS) at the Delft University of Technology. The subjects were seated in the right seat of the simulator, using an electric sidestick to give an input to the system. The stick was fixed in the pitch axis and could only rotate around its roll axis.

The displays were presented on the primary flight display of the simulator, directly in front of the subjects, with green lines and indicators on a black background. These displays were either compensatory or preview, as can be seen in Figure 1.

C. Control Variables

Two seconds of preview are displayed on the screen, well above the critical preview time found in [10]. The critical preview time is defined as the length of preview above which there is no improvement in the tracking performance.

The motion cue used in the experiment was the yaw rotation of the simulator, and was the same for all the conditions including motion feedback. The yaw rotation was corrected so that the motion axis was centered in the right seat of the simulator and not on the centroid of the simulator. Motion was presented one to one, without no washout.

D. Forcing Functions

To facilitate the use of system identification methods described in Section III-G, the forcing functions in the experiment were defined as a sum of sinusoids given by Equation (16). The same expression was used for the disturbance and target forcing functions.

$$f_{t,d}(t) = \sum_{k=1}^{20} A_{t,d}[i] \sin(\omega_{t,d}[i]t + \phi_{t,d}[i]) \tag{16}$$

In this expression, f stands for the forcing function signal, and A, ω and ϕ for the sinusoid amplitude, frequency and phase, respectively.

Both target and disturbance amplitudes were defined using a second-order low-pass filter, as used in [7]. The absolute value of the filter at a given frequency yields the sinusoid amplitude. This filter is defined in Equation (17).

$$H_A(j\omega) = \frac{(1 + 0.1j\omega)^2}{(1 + 0.8j\omega)^2} \tag{17}$$

This amplitude distribution results in a realistic and not too difficult task for the subjects [7]. This is also the same amplitude distribution used in previous yaw motion experiments, such as [4]. In order to avoid leakage and allow the use of spectral analysis, the frequencies used were integer multiples of the base frequency ω_b. Each run consisted of a measurement time of 120 seconds, which yields a base frequency $\omega_b = 2\pi/120 = 0.0524$ rad/s. To allow for the calculation of coherence, double bands of frequencies were used [8]. The frequencies used were the same as in [8] and [9], in a total of 20 sinusoids.

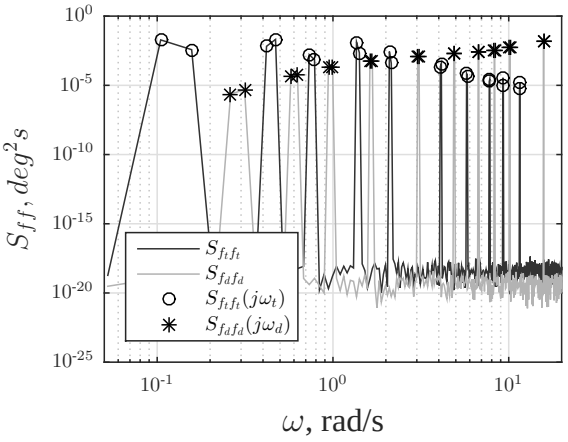

Fig. 5: Single-sided Power Spectral Density of the forcing function signals

Five different target signals were used, different only on the phases ϕ_t, to avoid memorization of the signal by the subjects. For the disturbance signal only one realization was used, as it is unlikely the subjects would memorize it since it is not directly displayed. Given that in the SRS the disturbance is inserted before the controlled element, it was pre-filtered with the inverse dynamics of the controlled element. The standard deviation of the target forcing function was 4.5 degrees and of the disturbance forcing function was 1.8 degrees. The spectra of the forcing function signals are shown in Figure 5.

E. Experimental Procedure

The experiment was performed by eight male volunteers aged between 22 and 32 years old. Their experience in tracking

tasks ranged from little practice to extensive experience. All the subjects were briefed before participating, and given all necessary instructions to perform the experiment.

For each subject, a task familiarization was performed before the actual experiment, in which each condition was tried at least once. After this phase, the measurement phase begun. The order of the conditions was randomized using a balanced Latin-Square distribution among the subjects. For each condition, each subject performed three training runs, and an extra five to twelve runs, until stable performance was achieved. Only the last five runs of each condition for each subject were used for data analysis.

After every run, the experimenter reported the score to the subjects, using the root-means-square of the error. Each run lasted for 132 seconds, of which the first eight seconds were run-in time and the last four were fade-out time, with 120 seconds being used as measurement time. Breaks were taken between every two conditions. The total experiment time, breaks included, was around three hours per subject.

F. Dependent Variables

In this experiment, the variances of the error and control output are used quantify performance and control activity. Coherence is calculated to validate the use of a quasi-linear model for the human controller. Open-loop describing functions are calculated in order to obtain crossover frequencies and phase margins to quantify performance in the frequency domain and closed-loop stability. Black-box identification and parameter estimation are used to obtain the frequency response of the human controller. Model parameters are obtained based on the proposed model in order to understand the human behavior in the control task. Model VAFs are obtained in order to quantify the ability of the model to describe the output.

G. Data Analysis

1) Coherence: The coherence is a measure for the linear relationship between two signals. It can range from 0 to 1, where 0 means no linear relation and 1 means completely linear relation. The coherence is calculated to verify the linearity of the human controller's inputs in response to the applied forcing functions. A high coherence shows that the relation is close to linear, which means that quasi-linear models can be applied to model the human controller dynamics REF. Equation (18) shows how coherence is estimated for the target signal. Calculation for the disturbance signal is analogous.

$$\Gamma_{f_t,u}(\tilde{\omega}_t) = \sqrt{\frac{|\tilde{P}_{f_t u}(\tilde{\omega_t})|^2}{\tilde{P}_{f_t f_t}(\tilde{\omega_t})\tilde{P}_{uu}(\tilde{\omega_t})}}, \tag{18}$$

In this equation, $\tilde{\omega}$ is the average frequency between two frequencies in a double band, and $\tilde{P}$ is the average periodogram of the respective subscripted signals at that average frequency.

2) Open-loop Describing Functions: Open-loop describing functions allow to further understand the performance and the stability of the system. The measures used are the crossover frequency ω_c, which corresponds to the frequency at which $|H_{ol}(j\omega)| = 1$, and the phase margin ϕ_m defined by $180 + \angle H_{ol}(j\omega_c)$. The open-loop describing functions are defined, for a combined target-tracking and disturbance-rejection tracking tasks, as in [12]:

$$\begin{aligned} H_{ol,t}(j\omega_t) =& \frac{X(j\omega_t)}{E(j\omega_t)} \\ =& \frac{H_{o_t}(j\omega_t)H_{ce}(j\omega_t)}{1 + [H_{o_x}(j\omega_t) - H_{o_t}(j\omega_t)]H_{ce}(j\omega_t)} \end{aligned} \tag{19}$$

$$\begin{aligned} H_{ol,d}(j\omega_t) =& \frac{X(j\omega_d) - F_d(j\omega_d)}{X(j\omega_d)} \\ =& H_{ce}(j\omega_d)H_{o_x}(j\omega_d) \end{aligned} \tag{20}$$

3) Black-Box Multiloop System Identification: For system identification, a black-box, Fourier coefficient based method is used, as described in [13]. For the introduced two-channel model (see Figure 4), Equation (21) can be obtained, in which U, F_t and X are the Fourier transforms of the control output, the target forcing function and the controlled element output, respectively. This equation excludes the remnant, as it is considered small at the input frequencies [13].

$$U(j\omega) = H_{o_t}(j\omega)F_t(j\omega) - H_{o_x}(j\omega)X(j\omega) \tag{21}$$

This equation contains two different describing functions, H_{o_t} and H_{o_x}. In order to solve for both describing functions, a second equation is required. This equation can be obtained by evaluating Equation (21) only at the signal input frequencies, while also interpolating the Fourier transforms at the disturbance frequencies to the target frequencies, yielding the signals $\tilde{U}$, $\tilde{F}_t$ and $\tilde{X}$. This yields a system of two equations and two unknowns, given by Equation (22), which can be solved for H_{o_t} and H_{o_x}. The same process is performed for the disturbance frequencies, so that H_{ot} and H_{ox} estimates are obtained at all excited frequencies.

$$\begin{bmatrix} U(j\omega_t) \\ \tilde{U}(j\omega_t) \end{bmatrix} = \begin{bmatrix} F_t(j\omega_t) & -X(j\omega_t) \\ \tilde{F}_t(j\omega_t) & -\tilde{X}(j\omega_t) \end{bmatrix} \begin{bmatrix} H_{o_t}(j\omega_t) \\ H_{o_x}(j\omega_t) \end{bmatrix} \tag{22}$$

4) Parameter Estimation: The model parameters were obtained by minimization of a cost function J, given in Equation (23).

$$J(\Theta) = \sum_{i=1}^{N_t} |U(j\omega_i) - \hat{U}(j\omega_i|\Theta)|^2 \tag{23}$$

with

$$\hat{U}(j\omega_i|\Theta) = \hat{H}_{o_t}(j\omega_i|\Theta)F_t(j\omega_i) - \hat{H}_{o_x}(j\omega_i|\Theta)X(j\omega_i) \tag{24}$$

This cost function is the difference between the measured and modeled control output, at a number N_t of ω_i frequencies below a cut-off frequency, chosen at 25 rad/s. The parameter vector Θ is defined as $[K_{e^\star}\ T_{L,e^\star}\ \tau_v\ \omega_{nms}\ \zeta_{nms}\ K_f\ T_{l,f}\ \tau_f,\ K_m,\ \tau_m]^{\mathrm{T}}$.

In order to minimize J, a Nelder-Mead algorithm was used, with the MATLAB function *fminsearch()*. It was constrained to discard only negative parameters. 10,000 initial parameter sets are randomly generated and the 100 with the lowest cost function are used as starting points for the optimization. The solution with the lowest cost is considered the best solution.

5) Variance Accounted For: The Variance Accounted For (VAF) is used as a measure of the similarity of two signals. A maximum value of 100% means that the signals are identical. It can then be used to compare the modeled and measured control output, to quantify how well the model represents the human controller behavior. The VAF is given by:

$$VAF = \left(1 - \frac{\sum_{k=1}^{N_s} P_{\epsilon_u \epsilon_u}(k\omega_b)}{\sum_{k=1}^{N_s} P_{uu}(k\omega_b)}\right) \times 100\%, \qquad (25)$$

with ϵ_u the modeling error ($U(j\omega_k) - \hat{U}(j\omega_k|\Theta)$) and N_s is the total number of samples.

6) Data Processing: Coherence was calculated per subject and per run. The results were averaged over five runs and then averaged over the eight subjects, for each condition. The variances of the error and control output were calculated for individual runs and averaged for each subject. These variances were calculated by integration of power spectral densities, in order to allow separation of the contributions of target, disturbance and remnant frequencies [12]. The frequency response functions were estimated using the frequency-domain average of the five measurement runs for each subject, in order to reduce noise. The phase margins and crossover frequencies were calculated using the estimated frequency response functions, using Equation (19) and (20). The Variance Accounted For is calculated per subject, based on the obtained models.

A two-way repeated measures ANOVA was applied to test for significant changes in tracking performance, control activity, crossover frequency and phase margin. 95% confidence intervals of the variances, crossover frequencies, phase margins and model parameters were corrected for between-subject variability.

IV. Results

A. Tracking Performance and Control Activity

Figure 6 shows the average variances of the tracking error e and the control output u, for each condition. Each bar also shows the contributions of the target, disturbance and remnant frequencies. The 95% confidence intervals of the means of the total σ_e^2 and σ_u^2 are also depicted.

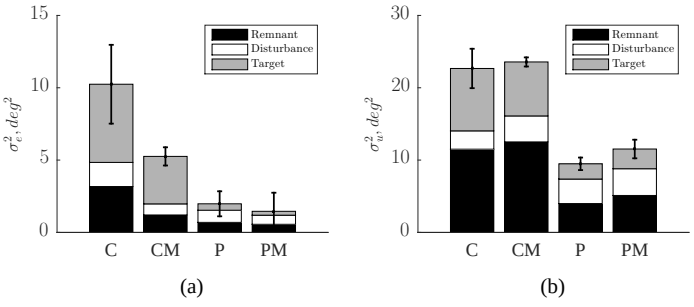

Fig. 6: Variance of the error (a) and control output (b)

A statistical test is performed in order to further understand how significant are the effects of the different displays and motion feedback for the error and control output variance.

TABLE II: Tracking performance and control activity ANOVA Results [1]

		error, e			control output, u		
		df	F	sig.	df	F	sig.
σ^2	motion	(1,7)	12.033	*	(1,7)	0.220	-
	display	(1,7)	44.264	**	(1,7)	14.559	**
	mot.*disp.	(1,7)	13.107	**	(1,7)	0.055	-
σ_t^2	motion	(1,7)	15.265	**	(1,7)	0.114	-
	display	(1,7)	89.992	**	(1,7)	84.244	**
	mot.*disp.	(1,7)	18.795	**	(1,7)	2.074	-
σ_d^2	motion	(1,7)	30.030	**	(1,7)	2.956	-
	display	(1,7)	35.639	**	(1,7)	0.805	-
	mot.*disp.	(1,7)	17.369	**	(1,7)	1.762	-
σ_n^2	motion	(1,7)	6.111	*	(1,7)	0.271	-
	display	(1,7)	12.342	*	(1,7)	9.414	*
	mot.*disp.	(1,7)	7.500	*	(1,7)	0.001	-

[1]The symbol - stands for not significant result (p>0.05), * for significant result (p<0.05) and ** for highly significant result (p<0.01)

When analyzing the error variances, there is a significant difference in performance for the target, remnant and disturbance contributions, both for motion and displays. This suggests that the extra information provided to the human controller effectively allows to control the system with a smaller error.

Preview yields a significant improvement in target performance, see Table II. This is most visible in the target frequencies, with a reduction in the error of 92%. With preview, humans can see the future target and anticipate its upcoming changes. There is a significant effect of the applied display variation for the target, disturbance and remnant frequencies on the tracking performance, which shows that preview information allows the human controller to improve both its target-tracking and disturbance-rejection performance.

Motion feedback also has a significant effect on tracking performance, which can be seen for all frequencies. This effect can be seen both for compensatory and preview displays. The motion effect exists for both displays, even though it is smaller in percentage for the preview display. This can be seen in the statistical results as a significant interaction of motion and display for target, disturbance and remnant frequencies tracking performance. This suggests human controllers indeed use motion feedback in preview tracking.

Regarding control activity, the statistical analysis indicates that only the display has a significant effect on the target frequencies. Because human controllers can distinguish between the target and disturbance signals on the preview display (and not on the compensatory display), they respond more linearly (less remnant) and they choose to respond less aggressively to the target signal. Figure 6. When preview is provided, without motion, there is a 58% decrease in the control activity, and a 33% increase in the disturbance control activity, which is not significant.

Motion feedback does not have a significant effect on the control activity. This can also be clearly seen in Figure 6,

in which the change in control activity variance between the motion and no motion condition are very small.

B. Coherence

The average coherence for each condition is shown in Figure 7 for the target frequencies and in Figure 8 for the disturbance frequencies.

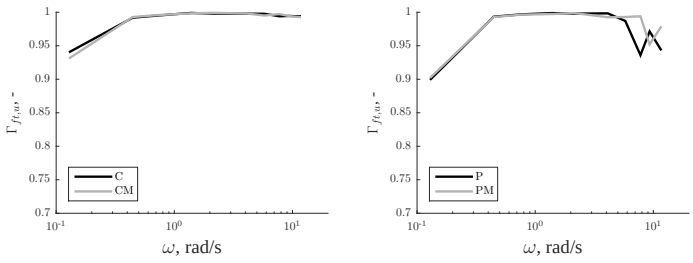

Fig. 7: Coherence between the target and control output signals, for the compensatory (a) and preview (b) tasks

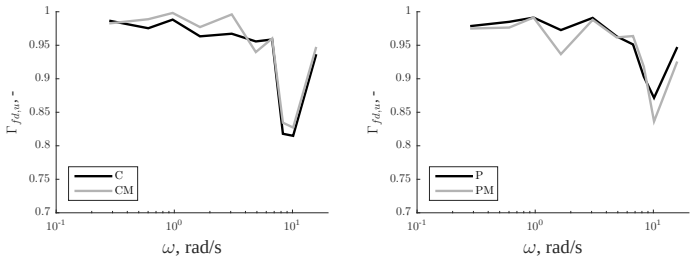

Fig. 8: Coherence between the disturbance and control output signals, for the compensatory (a) and preview (b) tasks

It is clear that all results are very close to 1, which validates the use of a quasi-linear model for the human. These results are 10 to 20 % higher, depending on the frequency, than what was found in previous preview tracking experiments [8], [10], which can be explained by the amplitude filter used in this experiment. The use of an amplitude filter reduces the power of the high frequencies of the signal, which makes the task easier for the human controller. It should also be noted that the disturbance coherence at the higher frequencies is smaller than the target coherence.

C. Crossover Frequency and Phase Margin

The crossover frequencies and phase margins are shown in Figures 9 and 10. In each figure, the results for each subject are presented, along with the mean of all subjects and the 95% confidence intervals of the means.

Figure 9 and 10 shows clear effect of both preview and motion feedback. On the one hand, preview significantly increases the target crossover frequency and phase margin. For target-tracking, preview allows the human to become more stable (increased phase margin), due to the ability to see the future target. The negative time delay present in the preview task provide phase lead to the human controller, which makes the system more stable. On the other hand, motion significantly increases the disturbance crossover frequency, as the disturbance task is easier for the human controller when using motion feedback. It should also be noted that there is an increase in the target crossover frequency when motion is added for the preview task, which is an indicator that motion feedback makes the task easier for the human controller. Neither motion feedback nor preview have a clear contribution to the disturbance phase margin, as can be seen in Figure 10(b), and indeed both effects are not significant, as seen in Table III.

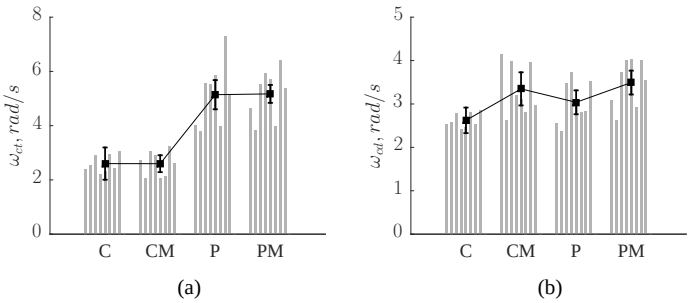

Fig. 9: Target (a) and disturbance (b) crossover frequency

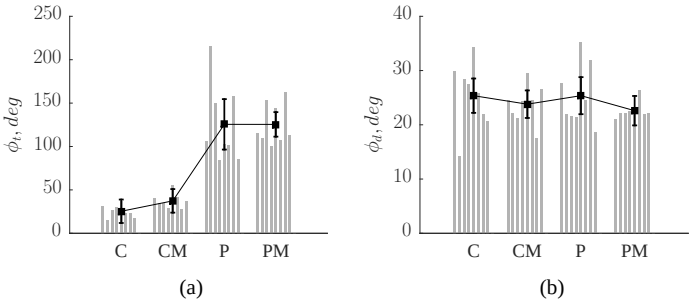

Fig. 10: Target (a) and disturbance (b) phase margin

TABLE III: CROSSOVER FREQUENCY AND PHASE MARGIN ANOVA RESULTS [2]

		target			disturbance		
		df	F	sig.	df	F	sig.
ω_c	motion	(1,7)	1.487	-	(1,7)	12.126	*
	display	(1,7)	39.044	**	(1,7)	2.401	-
	mot. * disp.	(1,7)	3.195	-	(1,7)	1.902	-
ϕ_m	motion	(1,7)	0.031	-	(1,7)	0	-
	display	(1,7)	82.872	**	(1,7)	1.079	-
	mot. * disp.	(1,7)	1.320	-	(1,7)	1.217	-

[2]The symbol - stands for not significant result (p>0.05), * for significant result (p<0.05) and ** for highly significant result (p<0.01)

D. Human Controller Describing Functions

Using the Black-Box identification method described in Section III-G, the human controller describing functions can be identified. The resulting Bode plots are shown in Figure 11 for subject 8 in the condition of preview with motion feedback.

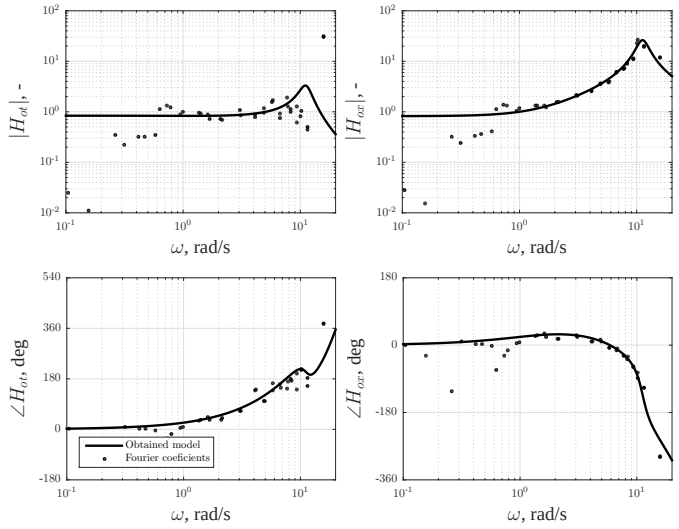

Fig. 11: Frequency response function for the preview task with motion feedback (subject 8)

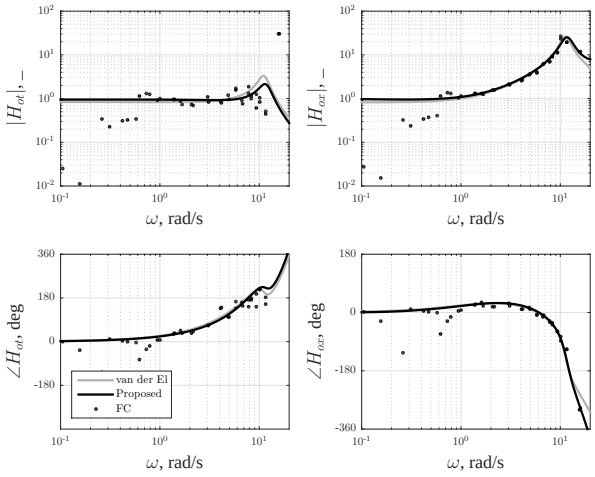

(a)

Fig. 12: Frequency response functions for Subject 8, fitted for the van der El model (VAF=92.38%) and the proposed model including motion feedback (VAF=92.79%).

E. Model comparison

Given the similarity between the models, it was decided to test both the original preview model proposed by van der El et. al [8] and the proposed model for the preview with motion feedback condition. Both models were fitted to the results of the preview with motion feedback condition (PM), in order to understand if the addition of the motion channel causes a significant difference in the Variance Accounted For, the frequency response function, or the parameters of the model. The obtained frequency response functions for both models are presented in Figure 12.

It can be seen in Figure 12 that there is not a significant difference between the two models. The visual channel of the van der El model is able to successfully model the entire response, with only a small change in the Variance Accounted For. The average model parameters are displayed in Table IV, along with the P results for reference.

TABLE IV: AVERAGE PARAMETER COMPARISON

	$K_e, -$	$T_{L,e}, s$	$\omega_{nms}, rad/s$	$\zeta_{nms}, -$	τ_v, s
P	0.52	1.14	11.40	0.17	0.24
PM van der El	0.87	0.68	11.95	0.21	0.18
PM Proposed	0.73	0.39	12.77	0.25	0.12
	$K_f, -$	$T_{l,f}, s$	τ_f, s	$K_m, -$	τ_m, s
P	0.92	0.57	0.77	-	-
PM van der El	1.00	0.70	0.68	-	-
PM Proposed	0.93	0.14	0.57	0.28	0.29

For the visual time delay τ_v and the lead time constant $T_{L,e}$, the notably lower values in the proposed model are caused by the interaction with the motion feedback path, as described in Section II-C. The far-viewpoint time constant $T_{l,f}$ seems to be the most affected by the change in these parameters.

The visual channel is then able to fully model the response, which is due to the similar function performed by the visual and motion channels in the proposed model. This fact reveals some ambiguity in the proposed model: even though it can fit the human response, it is an overdetermined model. The results for tracking performance and crossover frequency show that indeed there is a change in the human controller, but the proposed model does not correctly fit to the data using the identification techniques presented in this paper. We recommend further research on the separation of the motion and visual channels of the human controller, so that they can be uniquely identified and modeled. Considering these facts, the parameter estimation results obtained from the van der El *et. al* model [8], without the motion feedback channel will be used for the PM condition.

F. Human Controller Model Parameters

The model parameters, for the different conditions, can be seen in Figures 13-17. For each condition, the parameters are shown for each subject using gray bars, along with the mean of all subjects and the 95% confidence interval of the mean.

1) Error feedback response parameters: For both the error response gain $K_{e^\star}$ and lead time constant $T_{L,e^\star}$, the effect of motion feedback is similar for compensatory and preview displays. $K_{e^\star}$ increases when motion feedback is added, as the human responds more aggressively to the error. $T_{L,e^\star}$, on the other hand, shows a significant decrease, as the human controller is required to generate less lead in his visual

response. These results are consistent with previous work on compensatory tasks [4].

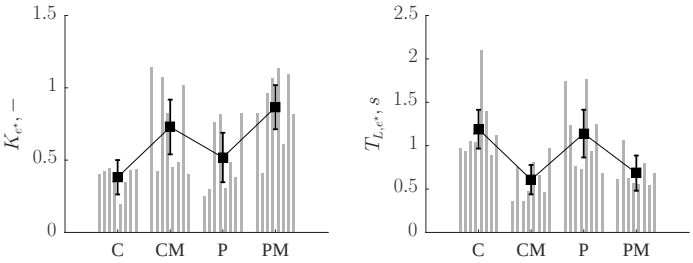

Fig. 13: Error response gain (a) and lead time constant (b)

2) Neuromuscular system parameters: Regarding the neuromuscular system parameters, motion feedback also has an important effect. There is an increase in the neuromuscular frequency ω_{nms} for both displays (see Figure 14(a)), with a 14% increase in the compensatory case and a 4% increase in the preview case. The increase for the compensatory task is according to what is commonly found in literature, [5], [4]. The neuromuscular damping ζ_{nms} registers a 21% increase for the compensatory case and a 25% increase for the preview case when motion is added.

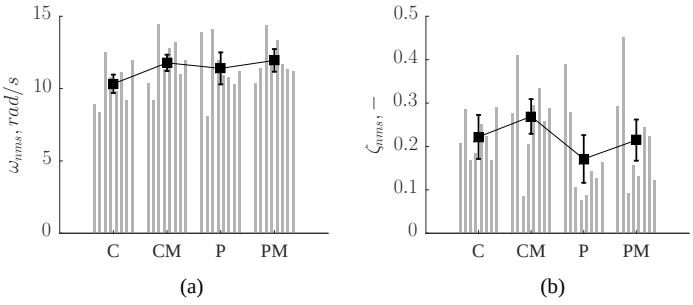

Fig. 14: Neuromuscular system parameters: natural frequency (a) and damping ratio (b)

3) Visual time delay: The visual time delay shows different effects for the compensatory and preview conditions. Using the compensatory display, when motion is added there is a 12% increase in the visual time delay, in line with what was reported in [4]. For the preview conditions, however, when motion is added there is a 24% decrease in the visual time delay.

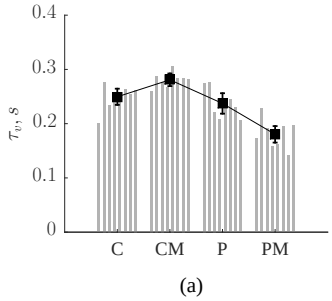

Fig. 15: Visual time delay

4) Far-viewpoint response parameters: The effect of motion feedback on the far-viewpoint gain K_f is small (see Figure 16(a)). It should also be noted that the parameter is extremely consistent across subjects and essentially a unit gain. The change in the far-viewpoint time-constant $T_{l,f}$ and position τ_f are also small, which suggest that motion feedback doesn't have a substantial effect in the way human controllers use preview.

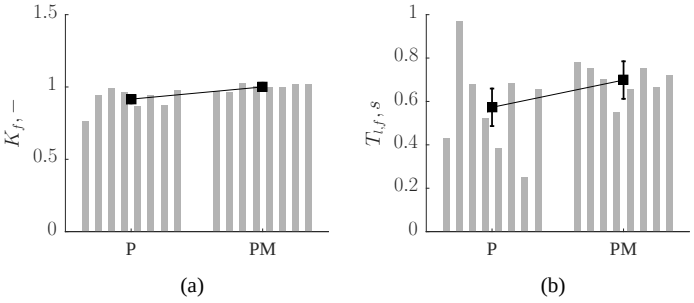

Fig. 16: Far-viewpoint gain (a) and lead time constant (b)

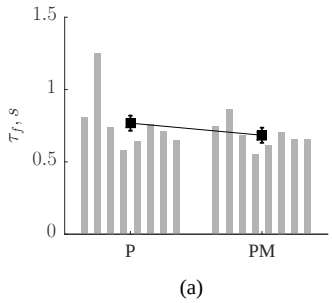

Fig. 17: Far-viewpoint position

G. Variance Accounted For

The obtained Variance Accounted For, shown in Figure 18 is well above 70% for all subjects in all conditions, which suggests the models used are an adequate representation of the human behavior. The proposed model for preview with motion feedback registers the lowest VAF found out of all model fits, with 75%, which is still a high value for this measure. In general, the model fits the experimental data well. The high

values for VAFs across conditions are also justified by the fact that the data was averaged in the frequency domain, as in [9].

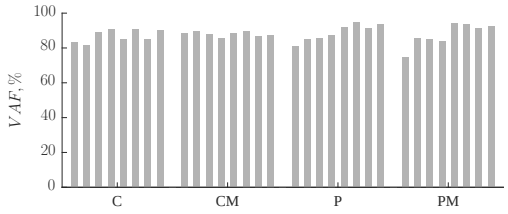

Fig. 18: Model VAFs per condition and subject

V. Discussion

In this paper, a human-in-the-loop tracking experiment was performed to study the role of motion feedback in preview tracking tasks in comparison with compensatory tracking.

Motion feedback allows humans to improve their performance in compensatory tracking tasks, which is consistent with many earlier investigations [3], [7], [5], [4]. Using motion feedback, humans are able to adapt their behavior, by controlling the system with an higher gain and being required to generate less lead. This result is thus highly consistent with compensatory literature.

When no motion feedback is present, preview allows humans to improve their performance significantly. The ability to see the future target allows humans to improve tracking performance. Human controllers respond to an internal error, filtered by the far-viewpoint response dynamics, as was found in the work of van der El *et. al* [8].

For preview tracking, the effect of motion is seemingly similar as in compensatory tracking. Motion still allows a significant improvement in performance, and the human adaptation is shown by an increase of the error response gain $K_{e^\star}$ and a decrease of the lead time constant $T_{L,e^\star}$. However, we were not able to prove the use of the additional motion channel H_{om}, due to the ambiguity of the proposed model. Motion does not cause a change in the way human controllers use preview parameters, with the far-viewpoint parameters registering only small changes. Control activity is not significantly affected by the availability of motion feedback, as found for the compensatory case.

Regarding the parameter estimation results, even though the proposed model is able to fit the data correctly, it is ambiguous regarding the parameters on the motion feedback loop. Based on this fact, we recommend further research that is able to clearly separate the visual and motion channels.

This paper successfully showed for the first time the role of motion feedback on preview tracking tasks: when preview information is available, human controllers are still able to adapt their control behavior and improve tracking performance, without a substantial change in control activity.

VI. Conclusion

This paper studied the effect of yaw motion feedback on human control behavior in preview tracking tasks. We proposed a new quasi-linear human controller model for visual and preview tracking tasks with an additional motion feedback channel. A human-in-the-loop tracking experiment was performed. Results show that motion feedback helps to improve performance similarly in preview tasks, as it does in compensatory tasks, with an increase in the error response gain and a reduction in the lead time constant. The target crossover frequency and phase margin are mostly influenced by preview, while the disturbance crossover frequency is mostly influenced by the motion feedback. With this research, the effects of motion feedback in preview were studied for the first time, effectively allowing to bridge the knowledge gap between compensatory tasks with motion and preview tasks, by showing that human controllers use motion feedback in preview tracking to adapt their control behavior.

References

[1] D.T. McRuer and H.R. Jex. A Review of Quasi-Linear Pilot Models. *IEEE Transactions on Human Factors in Electronics*, 8(3):231–249, 1967.

[2] Ruud J. A. W. Hosman. *Pilot's Perception and Control of Aircraft Motions.* PhD thesis, Delft University of Technology, Faculty of Aerospace Engineering, 1996.

[3] Ruud J. A. W. Hosman and J. C. van der Vaart. Effects of Vestibular and Visual Motion Perception on Task Performance. *Acta Psychologica*, 48:271–287, 1981.

[4] Tao Lu, Daan M. Pool, Marinus M. van Paassen, and Max Mulder. Use of Simulator Motion Feedback for Different Classes of Vehicle Dynamics in Manual Control Tasks. In *Proceedings of the 5th CEAS Air & Space Conference, Delft, The Netherlands*, number 52, September 2015.

[5] Daan M. Pool, Herman J. Damveld, Marinus M. van Paassen, and Max Mulder. Tuning Models of Pilot Tracking Behavior for a Specific Simulator Motion Cueing Setting. In *Proceedings of the AIAA Modeling and Simulation Technologies Conference, Portland, Oregon, Aug. 8-11*, number AIAA-2011-6322, 2011.

[6] Daan M. Pool, Gertjan A. Harder, and Marinus M. van Paassen. Effects of Simulator Motion Feedback on Training of Skill-Based Control Behavior. *Journal of Guidance, Control, and Dynamics*, 39(4):889–902, 2016.

[7] Peter M. T. Zaal, Daan M. Pool, Jaap de Bruin, Max Mulder, and Marinus M. van Paassen. Use of Pitch and Heave Motion Cues in a Pitch Control Task. *Journal of Guidance, Control, and Dynamics*, 32(2):366–377, 2009.

[8] Kasper van der El, Daan M. Pool, Herman J. Damveld, Marinus M. van Paassen, and Max Mulder. An Empirical Human Controller Model for Preview Tracking Tasks. *IEEE Transactions on Cybernetics*, 2015.

[9] Kasper van der El, Daan M. Pool, Marinus M. van Paassen, and Max Mulder. How Human Controllers use Preview to Improve Target-Tracking Performance. *IEEE Transactions on Cybernetics*, 2016.

[10] Sharon Padmos, Kasper van der El, Daan M. Pool, Herman J. Damveld, Marinus M. van Paassen, and Max Mulder. The effect of preview time on human control behavior in rate and acceleration tracking tasks. *In preparation*, 2016.

[11] Daan M. Pool, Ana Rita Valente Pais, Aniek M. de Vroome, Marinus M. van Paassen, and Max Mulder. Identification of Nonlinear Motion Perception Dynamics Using Time-Domain Pilot Modeling. *Journal of Guidance, Control, and Dynamics*, 35(3):749–763, May–June 2012.

[12] Henry R. Jex, R. E. Magdaleno, and Andrew M. Junker. Roll Tracking Effects of G-vector Tilt and Various Types of Motion Washout. In *Proceedings of the Fourteenth Annual Conference on Manual Control*, pages 463–502, 1978.

[13] Marinus M. van Paassen and Max Mulder. Identification of Human Operator Control Behaviour in Multiple-Loop Tracking Tasks. In *Proceedings of the Seventh IFAC/IFIP/IFORS/IEA Symposium on Analysis, Design and Evaluation of Man-Machine Systems, Kyoto Japan*, pages 515–520. Pergamon, 1998.